Science Advances
AAAS

Supplementary Materials for

Warmer temperatures favor slower-growing bacteria in natural marine communities

Clare I. Abreu *et al.*

Corresponding author: Clare I. Abreu, cabreu@stanford.edu; Martina Dal Bello, dalbello@mit.edu; Jeff Gore, gore@mit.edu

Sci. Adv. **9**, eade8352 (2023)
DOI: 10.1126/sciadv.ade8352

This PDF file includes:

Supplementary Text
Figs. S1 to S14
Table S1
References

Supplementary Text

I. Logistic and Lotka-Volterra competition models predict that increasing temperature favors the slower grower by decreasing mortality burden

In this paper, we expand upon previous theoretical and experimental results in which we showed that increasing temperature generally favored slower-growing species in pairwise competitions (*40*). To explain this result mathematically, we employed the two-species Lotka-Volterra (LV) interspecific competition model. The most basic form of the two-species Lotka-Volterra model takes the following form:

$$\frac{\dot{N}_i}{N_i} = r_i - c_{ii}N_i - c_{ij}N_j \quad (1)$$

where r_i is the exponential growth rate of species i (minus any intrinsic death rate), c_{ii} is the rate at which species i inhibits itself, and c_{ij} is the rate at which species j inhibits species i. Equation (1) can be re-parameterized to:

$$\frac{\dot{N}_i}{N_i} = r_i\left(1 - \frac{N_i - \beta_{ij}N_j}{K_i}\right) \quad (2)$$

where $K_i = \frac{r_i}{c_{ii}}$ is the carrying capacity and $\beta_{ij} = \frac{c_{ij}}{cii}$ is the competition coefficient. If the two species grow separately or do not interact, we set $\beta_{ij} = 0$ and the Lotka-Volterra model reduces to the logistic growth model:

$$\frac{\dot{N}}{N} = r\left(1 - \frac{N}{K}\right) \quad (3)$$

We will now compare the effect of temperature on two species growing independently before returning to interacting species in the Lotka-Volterra model.

Many microbial communities experience mortality that is not driven by competition and which affects the entire community. Importantly, this is true of all laboratory cultures, where cells are removed from the community either continuously (as in a chemostat or turbidostat) or at discrete intervals (as in batch culture). It may also result from predation by bacterivores, or, in the case of our gut microbiota, from waste passing through. Equation (3) can therefore be made more realistic by the introduction of a community-wide mortality rate (δ):

$$\frac{\dot{N}}{N} = r\left(1 - \frac{N}{K}\right) - \delta \quad (4)$$

Equation (4) can be reparametrized with modified carrying capacity $\widetilde{K} = K\left(1 - \frac{\delta}{r}\right)$ and growth rate $\tilde{r} = r - \delta$:

$$\frac{\dot{N}}{N} = \tilde{r}\left(1 - \frac{N}{\widetilde{K}}\right) \quad (5)$$

The effective carrying capacity $\widetilde{K}$ is modified by the ***mortality burden*** $\frac{\delta}{r}$, as mortality decreases the optimal carrying capacity. To determine how mortality burden affects the balance of two species, a slower-growing one N_s and a faster-growing one N_f, we can compute the ratio of their effective carrying capacities:

$$\frac{\widetilde{K}_s}{\widetilde{K}_f} = \frac{K_s}{K_f}\frac{\left(1-\frac{\delta}{r_s}\right)}{\left(1-\frac{\delta}{r_f}\right)} \tag{6}$$

How the ratio of effective carrying capacities changes across a temperature range determines how the balance of the two species changes with temperature. Since Equation (6) is a function of growth and death rates, the outcome will shift along with these rates. For example, the faster grower is favored by an increasing death rate (*61*). An increasing temperature, on the other hand, will affect growth rather than death. If we assume that maximal growth rates $r_i(T)$ are the only parameters affected by changes in temperature, we can take the derivative of Equation (6) with respect to temperature to see which species will benefit from an increase in temperature:

$$\frac{\partial}{\partial T}\frac{\widetilde{K}_s}{\widetilde{K}_f} = \frac{K_s}{K_f}\frac{\partial}{\partial T}\left(\frac{1-\frac{\delta}{r_s(T)}}{1-\frac{\delta}{r_f(T)}}\right) \tag{7}$$

We must choose a model for $r(T)$ in order to continue. As discussed in the main text, we use the Arrhenius equation:

$$r(T) = ae^{-\frac{E_a}{k_B T}} \tag{8}$$

where a is a pre-factor with dimensions of 1/time, E_a is the activation energy (in units of eV), k_B is the Boltzmann constant, and T is the temperature (in Kelvin). In the following equations, we will specify the fast grower with $r_f = a_f e^{-\frac{E_f}{k_B T}}$ and similarly for the slow grower. Plugging this form into Equation (7), we find:

$$\frac{\partial}{\partial T}\frac{\widetilde{K}_s}{\widetilde{K}_f} = \frac{K_s}{K_f}\frac{\frac{E_s}{k_B}\delta e^{\frac{E_s}{k_B T}}}{a_s T^2\left(1-\frac{\delta}{a_f e^{-\frac{E_f}{k_B T}}}\right)} - \frac{\frac{E_f}{k_B}\delta e^{\frac{E_f}{k_B T}}\left(1-\frac{\delta}{a_s e^{-\frac{E_s}{k_B T}}}\right)}{a_f T^2\left(1-\frac{\delta}{a_f e^{-\frac{E_f}{k_B T}}}\right)^2} \tag{9}$$

For the slow grower to be favored, the above term should be greater than zero, because this would mean that the ratio of the slow grower abundance to the fast grower abundance increases with temperature:

$$\frac{\frac{E_s}{k_B}\delta e^{\frac{E_s}{k_B T}}}{a_s T^2\left(1-\frac{\delta}{a_f e^{-\frac{E_f}{k_B T}}}\right)} > \frac{\frac{E_f}{k_B}\delta e^{\frac{E_f}{k_B T}}\left(1-\frac{\delta}{a_s e^{-\frac{E_s}{k_B T}}}\right)}{a_f T^2\left(1-\frac{\delta}{a_f e^{-\frac{E_f}{k_B T}}}\right)^2} \tag{10}$$

We can simplify this expression by plugging in r_f and r_s where they appear:

$$\frac{E_s}{r_s T^2\left(1-\frac{\delta}{r_f}\right)} > \frac{E_f\left(1-\frac{\delta}{r_s}\right)}{r_f T^2\left(1-\frac{\delta}{r_f}\right)^2} \tag{11}$$

Ultimately, the expression simplifies to a simple relation showing that the slow grower is always favored as temperature increases when the activation energies of the two species are the same (i.e. when $E_s = E_f$):

$$\frac{E_s}{E_f} > \frac{r_s-\delta}{r_f-\delta} \tag{12}$$

In the main text, we assumed equal activation energies of all species, and that differences in growth rates arise from differing rRNA copy numbers (which were absorbed into the pre-factor a). Thus, the inequality is always true under our assumptions.

The same result can be generated from the Lotka-Volterra model with two interacting species. We first re-parameterize the model by normalizing by carrying capacity:

$$\frac{\dot{\widehat{N}}_\iota}{\widehat{N}_\iota} = r_i\left(1-\widehat{N}_\iota-\alpha_{ij}\,\widehat{N}_{ij}\right) \tag{13}$$

where $\widehat{N}_\iota = \frac{N_i}{K_i}$ and $\alpha_{ij} = \beta_{ij}(\frac{K_j}{K_i})$. α_{ij} is a dimensionless competition coefficient quantifying the inhibition of species i by species j. The outcomes of the model are completely determined by the competition coefficients: when both $\alpha_{ij} < 1, \alpha_{ji} < 1$, both species coexist; when $\alpha_{ij} < 1$ but $\alpha_{ji} > 1$, species i drives species j to extinction (and vice versa); when both $\alpha_{ij} > 1, \alpha_{ji} > 1$, the result is bistability, in which both species can drive each other extinct, and the winner depends on the initial relative fraction. Thus, the model does not depend on the growth rates—a

strongly competing slow grower can drive a fast grower extinct. Introducing a community-wide mortality rate (δ), however, changes this:

$$\frac{\dot{\widehat{N}}_i}{\widehat{N}_i} = r_i\left(1 - \widehat{N}_i - \alpha_{ij}\,\widehat{N}_{ij}\right) - \delta \tag{14}$$

Equation (14) can be re-parameterized back into is original form, such that the outcome is determined completely by the re-parameterized competition coefficients $\tilde{\alpha}_{ij}$:

$$\frac{\dot{\widetilde{N}}_i}{\widetilde{N}_i} = \tilde{r}_i\left(1 - \widetilde{N}_i - \tilde{\alpha}_{ij}\widetilde{N}_j\right) \tag{15}$$

$$\tilde{\alpha}_{ij} = \alpha_{ij}\frac{\left(1 - \frac{\delta}{r_j}\right)}{\left(1 - \frac{\delta}{r_i}\right)} \tag{16}$$

Since $\tilde{\alpha}_{ij}$ is a function of growth and death rates, and with the same form as in the logistic model (Equation 6), the outcome will shift in the same way, favoring the slower grower as temperature increases.

We can repeat this calculation with another model for the dependence of growth rate on temperature. The Ratkowsky model (*83*) is consistently the best fit for microbial data:

$$r(T) = b^2(T - T_o)^2 \tag{13}$$

Where b and T_o must be determined by fitting data for a particular species. Repeating the calculation in the same way as above, we find a similar inequality that determines when the slow grower is favored by increasing temperature:

$$\frac{\left(T - T_{of}\right)}{\left(T - T_{os}\right)} > \frac{r_s - \delta}{r_f - \delta} \tag{14}$$

When the growth curves do not cross, we can assume that $T_{os} > T_{of}$ and $r_f > r_s$. These assumptions make the left side of the inequality greater than one, while the right side is less than one. Thus, the inequality is always true for a competition between a consistent slow grower and a consistent fast grower, and the LV model predicts that an increasing temperature will always favor a slower grower, provided that the slower grower does not become relatively faster at high temperature.

II. Modern coexistence theory analysis shows effect of temperature can be equalizing but not stabilizing

Modern coexistence theory defines two parameters that determine whether two species will coexist: niche overlap (ρ) and fitness ratio (f_2/f_1) (*59*). Coexistence can be favored by decreasing niche overlap or decreasing fitness differences. Mechanisms that decrease overlap are *stabilizing*, while those that decrease fitness differences are *equalizing*.

In the two-species Lotka-Volterra competition model, these parameters are defined as follows (*60*):

$$\rho = \sqrt{\frac{\alpha_{12}\alpha_{21}}{\alpha_{11}\alpha_{22}}} \tag{15}$$

$$\frac{f_2}{f_1} = \sqrt{\frac{\alpha_{11}\alpha_{12}}{\alpha_{21}\alpha_{22}}} \tag{16}$$

Equations (15)-(16) include intra-species competition coefficients α_{11} and α_{22} in addition to inter-species coefficients α_{12} and α_{21}. As described above in Supplementary Text I, we have parameterized the model to absorb the intra-species coefficients into the inter-species coefficients, and without loss of generality, we can set both $\alpha_{11} = 1, \alpha_{22} = 1$. Therefore Equations (15)-(16) become:

$$\rho = \sqrt{\tilde{\alpha}_{12}\tilde{\alpha}_{21}} \tag{16}$$

$$\frac{f_2}{f_1} = \sqrt{\frac{\tilde{\alpha}_{12}}{\tilde{\alpha}_{21}}} \tag{17}$$

where the modified coefficients $\tilde{\alpha}$ are defined by Equation (6).

In the case of a fast grower and a slow grower, we have shown above that, under our assumptions, $\frac{\partial}{\partial T}\tilde{\alpha}_{fs} > 0$ and $\frac{\partial}{\partial T}\tilde{\alpha}_{sf} < 0$. The ratio of the slow grower's fitness to the fast grower's fitness thus increases with temperature, leading to (dis)equalizing effects as temperature increases.

On the other hand, the niche overlap does not change with temperature, since the increase of $\tilde{\alpha}_{fs}$ matches the decrease of $\tilde{\alpha}_{sf}$, leading to no net change as temperature increases.

In the model, changes in temperature can therefore have (dis)equalizing but not (de)stabilizing effects upon species coexistence.

Fig. S1.

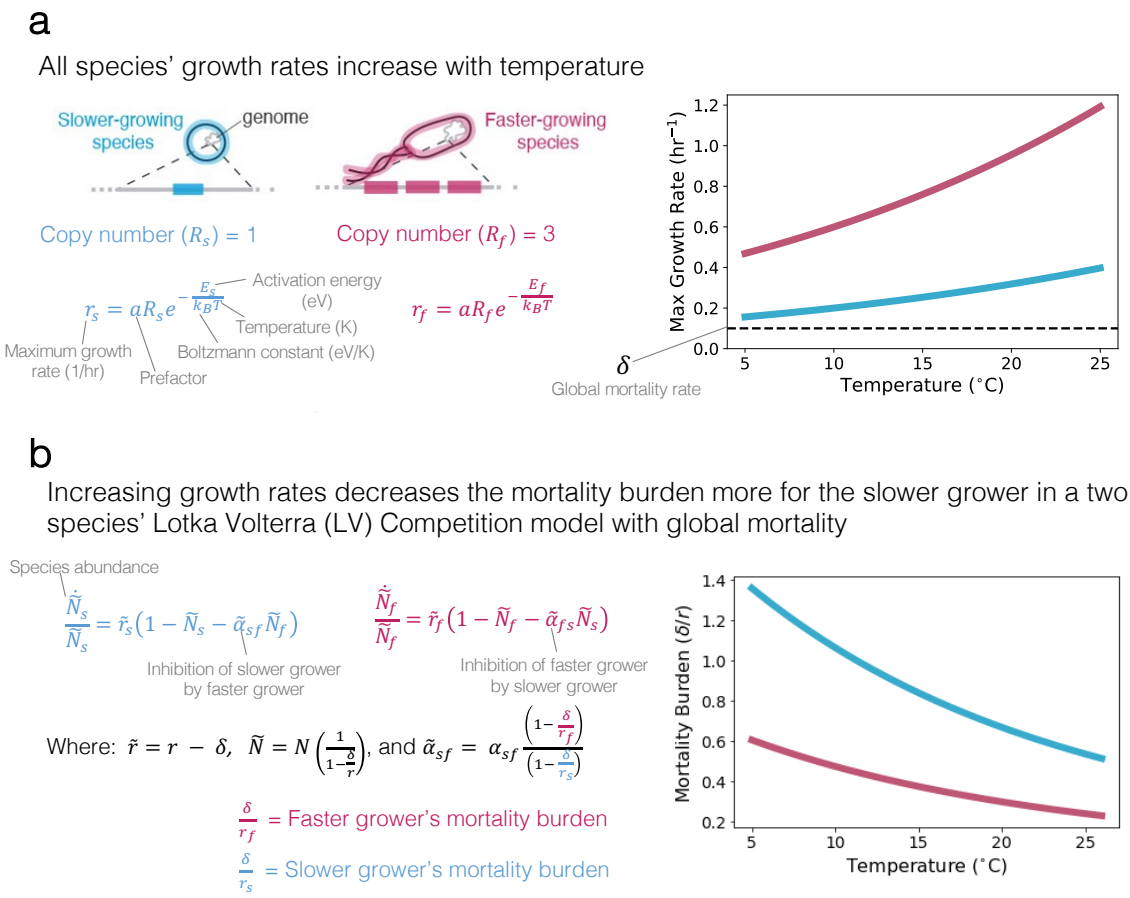

Two-species Lotka-Volterra competition model predicts that increasing temperature favors the slower grower. a. Bacterial maximum growth rates increase with temperature and are proportional to 16S ribosomal RNA operon copy number. The plot shows an example of two species' maximum growth rates over a temperature range of 20 °C, where the blue species has a single rRNA operon copy, and the pink species has 3 copies. **b**. The outcome of interspecies

competition in a two-species competitive Lotka Volterra model depends on the burden that mortality relatively imposes on the net growth rate of each species, quantified by δ/r , and therefore it can be modulated by changing the mortality rate or the growth rates of the species. In the plot, we show that the mortality burden decreases more for the slower grower than for the faster grower as growth rates increase driven by temperature, reducing the inhibition of the slower-grower by the faster-grower. **c**. The two-species competitive Lotka Volterra model presented in b., the abundance of the slow-grower increases with temperature. The MCN of the two-species community, as such, decreases from 3 at low temperature where the fast-grower excludes the slow-grower, to 1 at high temperature, where the slow-grower dominates. The analytical solutions are shown for the case in which $r = aRe^{-\frac{G}{T}}$, where $G = 3864$ and $a = 1.7e5$ for both species, and $R = 1$ for the blue species and $R = 3$ for the pink species.

Fig. S2.

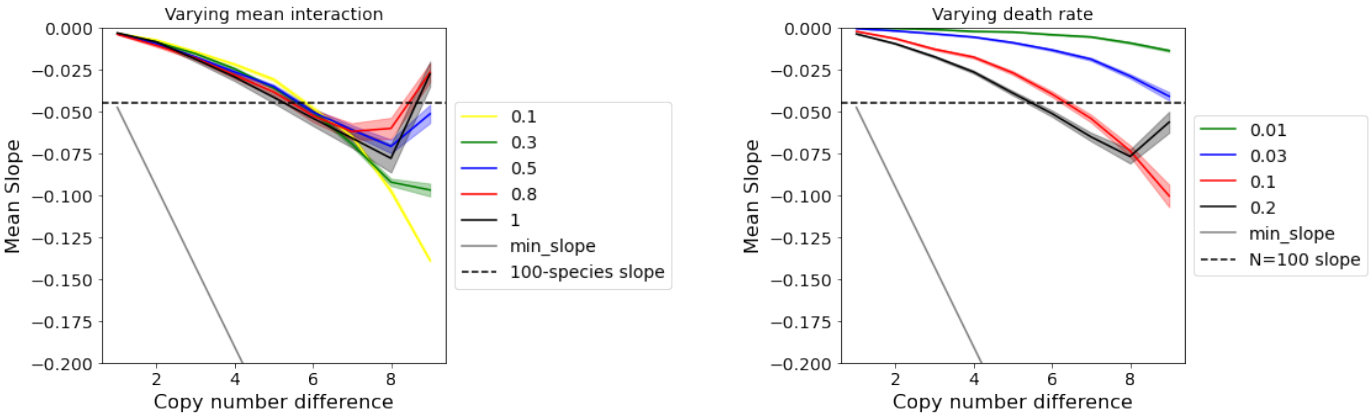

Two-species Lotka-Volterra solution is independent of mean interaction coefficient, as seen in the left plot. (Noise on the right end of the plot reflects extreme differences in copy number between the two species leading to fewer instances of coexistence and shallower MCN-temperature slopes.) The two-species solution is sensitive to death rate, with increasing death rate leading to steeper MCN-temperature slopes.

Fig. S3.

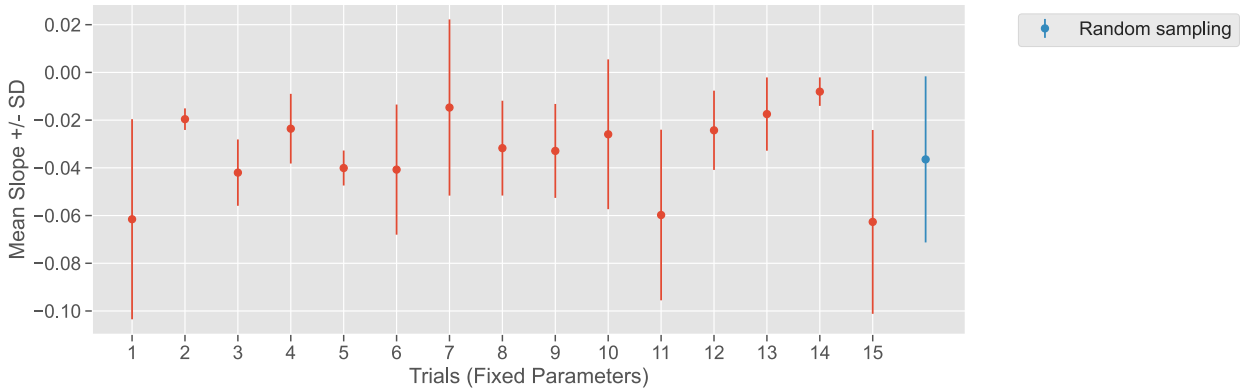

The mean and standard deviation of MCN-temperature slopes resulting from constant parameter simulations are similar to the mean and standard deviation of simulations performed by randomly sampling parameters. Red points represent randomly chosen parameters that remained fixed over 500 simulations (interaction coefficient matrices α_{ij} are unique for each simulation, even if mean interaction is fixed). The blue point on the right represents 500 simulations in which parameters were randomly sampled at each simulation (the mean of the normal distribution of α_{ij} was randomly drawn from a uniform distribution [0.1, 1] and the standard deviation was set to half the mean; the geometric distribution parameter p of the rRNA copy numbers was drawn from a uniform distribution [0.6, 0.9]; the mortality rate δ was drawn from a uniform distribution [0.03, 0.2]; the activation energy E was drawn from a uniform distribution [0.1 eV, 0.6 eV]).

Fig. S4.

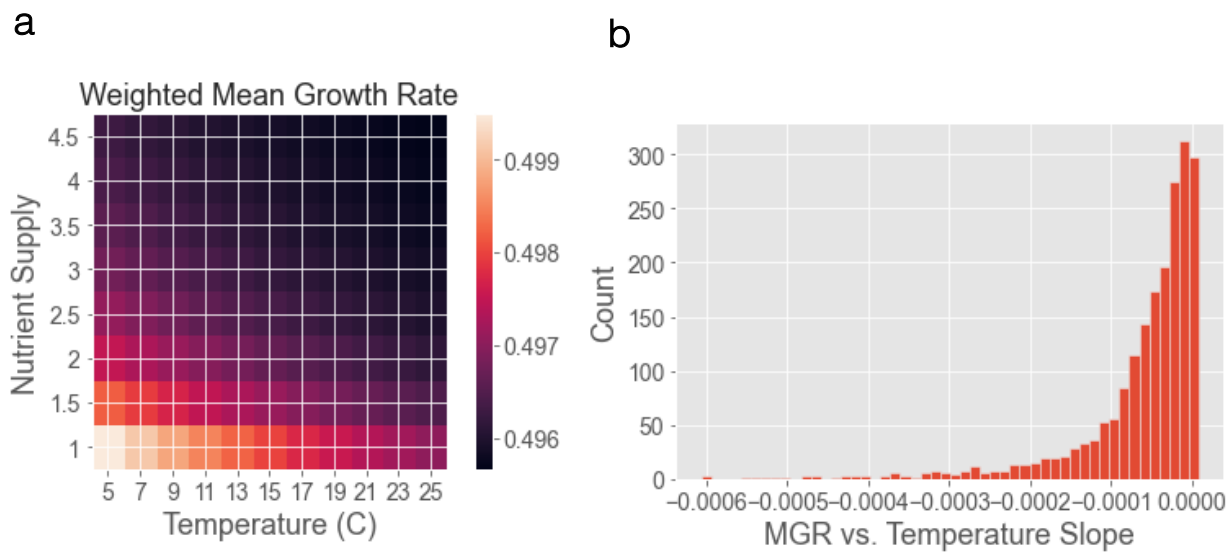

Consumer resource model predicts that warmer temperatures favor slower growers. As in the Lotka-Volterra model, increasing mortality and decreasing temperature favor fast growers with higher maximum growth rates, while slow growers benefit from decreasing mortality and increasing temperature. Panel **a** shows the weighted mean growth rate (MGR) of a community of fifteen species and ten resources, averaged over 250 simulations for 1000 hours in each temperature/nutrient supply combination. MGR is the average maximum growth rate of a community at a stable point weighted by the abundances of its members, where maximum growth rate is defined at a fixed temperature. Panel **b** plots all slopes of MGR over temperature, not just the average, to show that the majority of cases are negative. See Materials and Methods for details of model. Note that in this model, where growth rate increases linearly with resource concentration and no trade-offs are implemented, slower growers are also favored by an increase in nutrient supply. Including a trade-off between growth and affinity or adding other complications to the model might change this result.

Fig. S5.

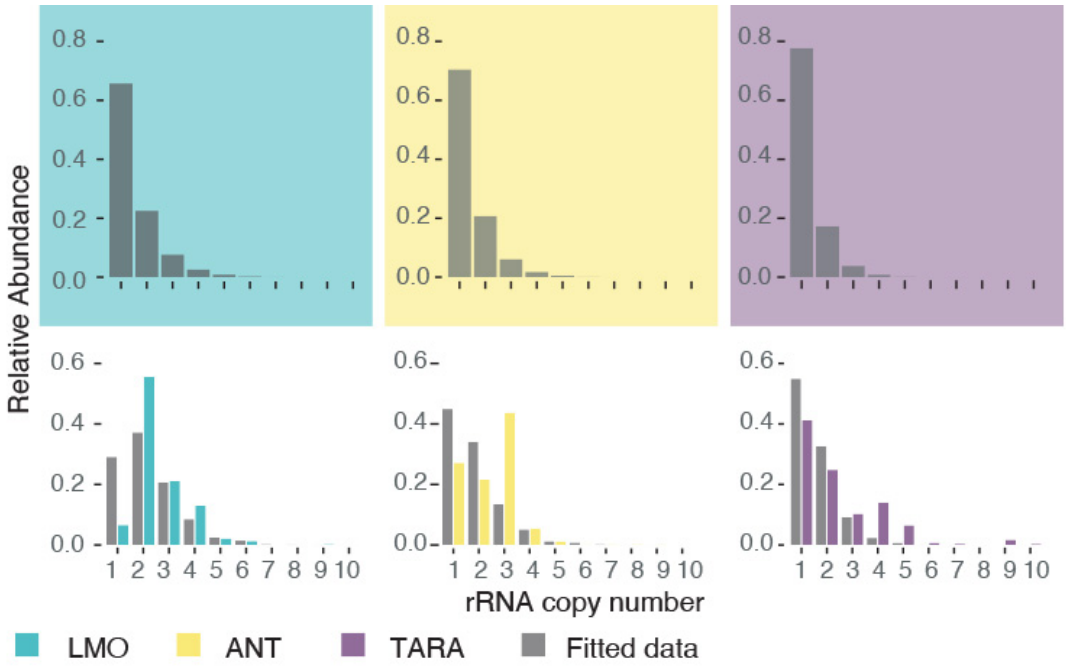

The final abundance distribution of copy numbers obtained from fitting the GLV model to data resembles the observed one in the three main datasets. Upper panels: abundance distribution of copy numbers the initialized communities in the model. Lower panels: abundance distribution of the equilibrated communities (grey) compared to the observed distribution of copy numbers in the three main datasets (green, LMO; yellow, ANT; purple, TARA).

Fig. S6.

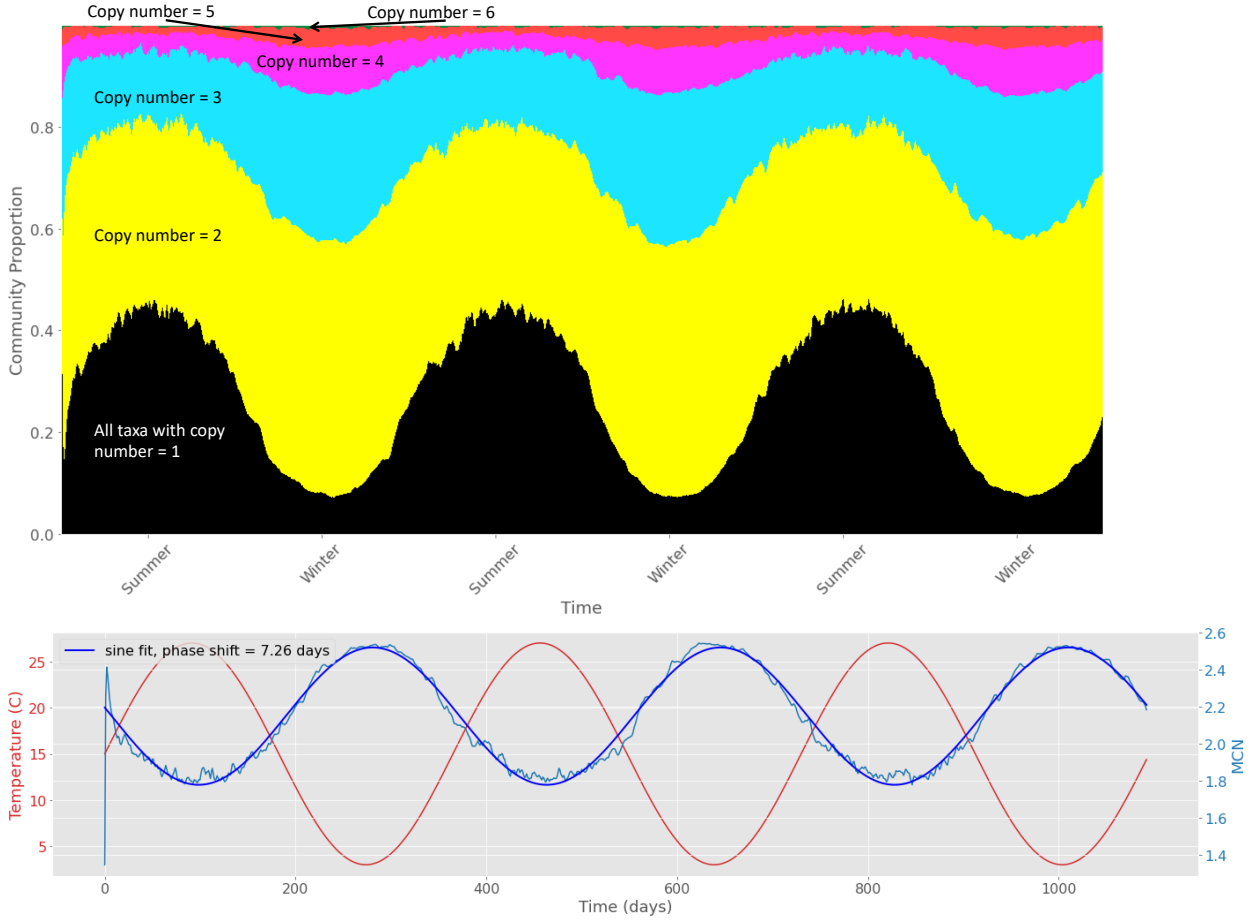

A continuous-time simulation with sinusoidally oscillating temperature shows that mean copy number (MCN) oscillations lag behind temperature oscillations, resulting in a frequency equal to that of temperature but with a phase shift of about one week (7.26 days) when the MCN was fit to a sinusoidal curve. The average of 50 Lotka-Volterra simulations is plotted, each with 100 species and mean interaction $\alpha = 0.5$ ($\sigma = 0.25$), mortality rate $\delta = 0.07/hr$, with copy numbers drawn from a geometric distribution, $p(1-p)^{R-1}$, where copy numbers R range from 1 to 10 and $p = 0.75$. Maximum growth rates are equal to $aRe^{-\frac{G}{T}}$, where R is the copy number, a is a prefactor equal to 170,000, the activation energy $G = 3864$, and temperature ranges from 3 to $27°C$. The simulations began with all species at equal relative abundance, and every four days, an abundance of 10^{-4} of all species (in units of fraction of single-species carrying capacities in the model) was added to the pool to represent migration and to prevent extinction.

Fig. S7.

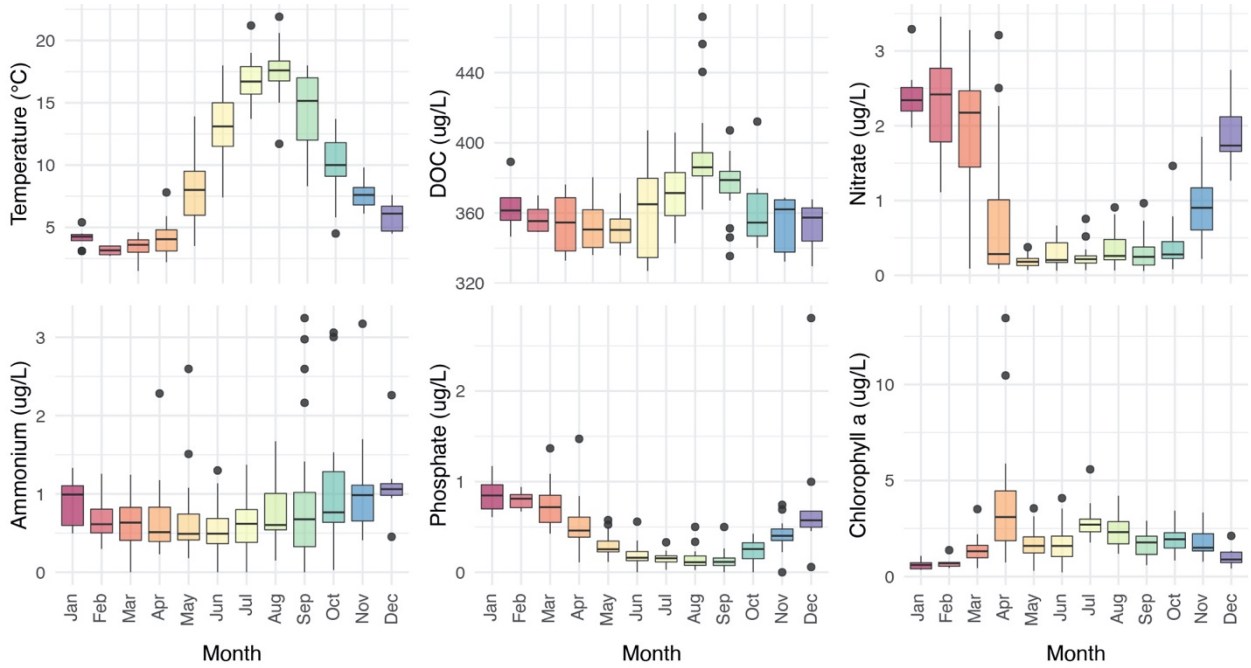

Many environmental variables show seasonality at the LMO station. Boxplots showing monthly variation in the environmental variables collected at the LMO station in 8 years (2011-2018).

Fig. S8.

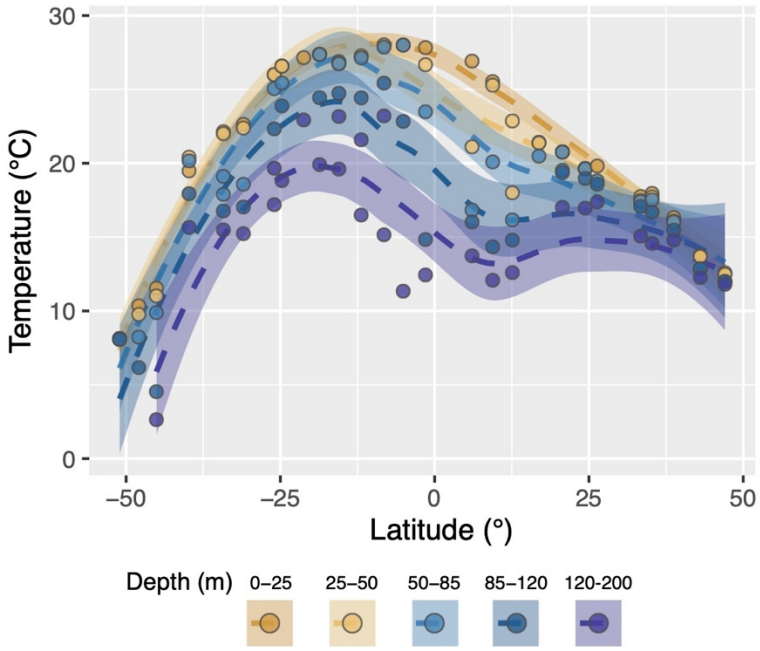

Temperature profiles at different depths show similar latitudinal trends at ANT sampling stations. Temperature variations across latitudes in the ANT dataset (dots, observed values, dashed lines: smoothing splines). Colors represent the depth range at which the sample was taken (five within the surface and the 200m).

Fig. S9.

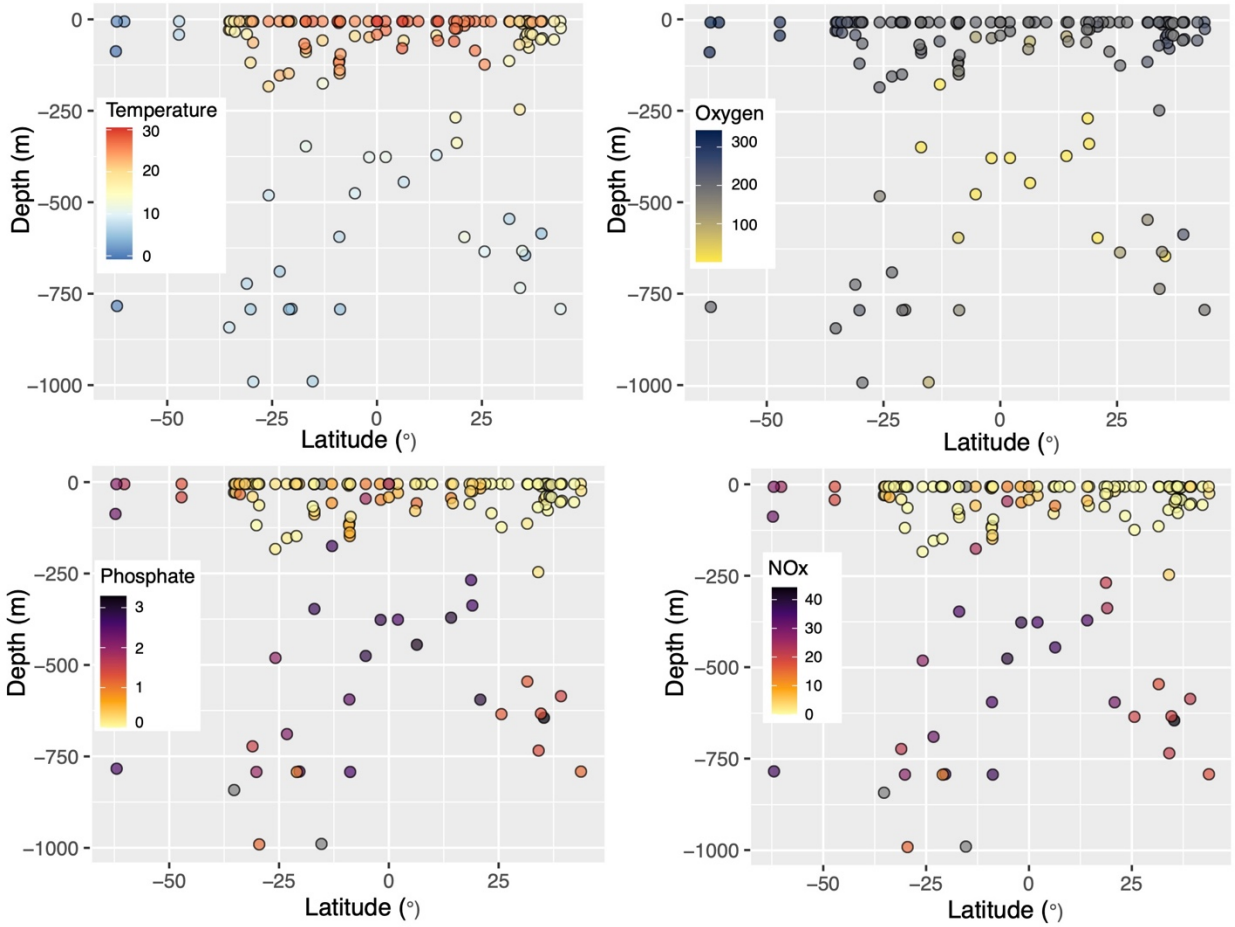

Temperature and oxygen decrease at high latitudes and with depth, while inorganic nutrients show the opposite pattern. Observed Temperatures, Oxygen, Phosphate and Nitrate + Nitrite (NOx) concentrations across latitudes and depths sampled in the TARA Ocean project.

Fig. S10.

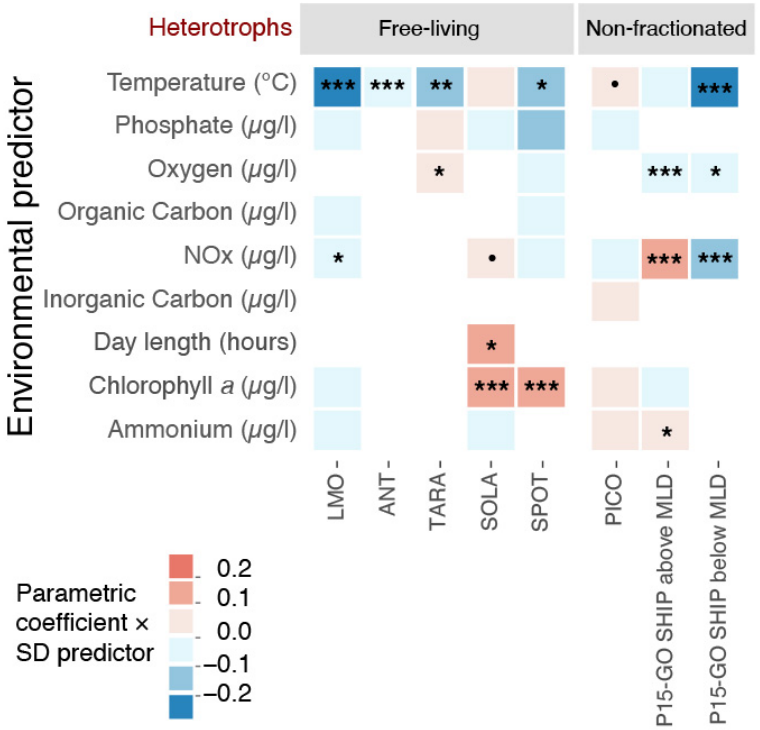

Considering the effect of primary productivity does not affect the negative effect of temperature on the distribution of fast and slow growing heterotrophs. Chlorophyll *a* concentration is a proxy for primary productivity and a known driver of several bacterial species (*6*, *75*). Since phototrophic bacteria contain chlorophyll *a*, they must be excluded from the calculation of the MCN to show that the temperature effect is robust to the inclusion of chlorophyll *a* concentration in the multiparametric analyses, which we do for the LMO and SPOT datasets (table S1, but see the results for SOLA time series in table S1). This analysis reveals that primary productivity is an important driver of the distribution of fast and slow-growing heterotrophic free-living bacteria in the SOLA and SPOT time series, promoting statistically significant increases in community MCN. In the case of LMO, instead, primary productivity did not exert a statistically significant effect on MCN. The temperature coefficient, however, remained negative and statistically significant in both SPOT and LMO, suggesting that the effect of temperature on bacterial community structure is independent of the effect of nutrient input rates. In the case of SOLA time series, the temperature effect was the weakest observed and it weakened further when primary productivity was considered, possibly due to the small seasonal thermal excursion in the Bay of Banyuls compared to the other time series and transects. Results for non-fractionated samples are more idiosyncratic. The figure shows a summary of the results of the multi-parametric regression on MCN of heterotrophic communities of all the datasets included in the study (free-living and non-fractionated samples). Tile colors represent the magnitude and sign of the parametric coefficient estimated for each available environmental variable multiplied by its standard deviation. Statistical significance of the parametric coefficients estimated through the models is indicated by symbols: '***' 0.001 '**' 0.01 '*' 0.05 '.' 0.1 ' ' 1.

Fig. S11.

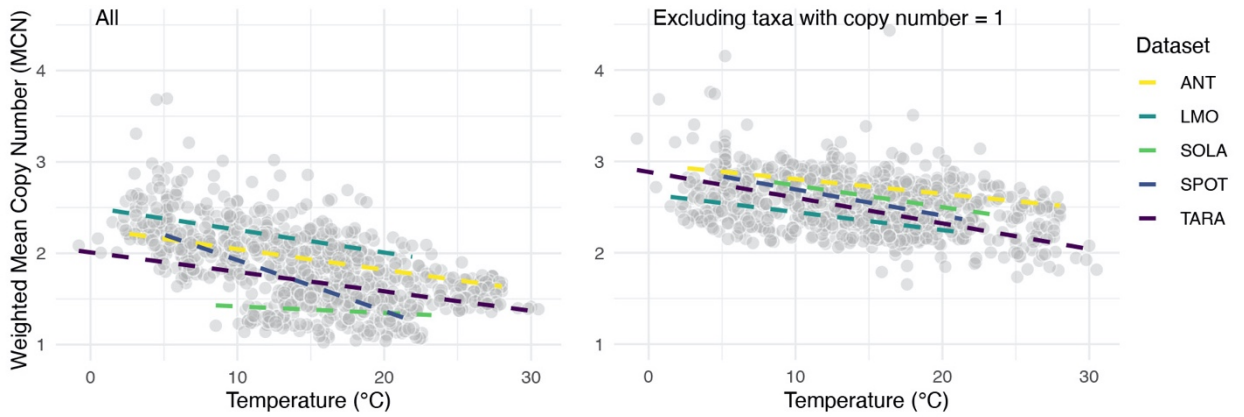

The relative abundance of free-living slow-growers increases with temperature, regardless of whether oligotrophs are included in the estimation of the weighted mean copy number (MCN) or excluded from it. Left panel: MCN calculated on all taxa; right panel: MCN calculated excluding taxa with copy number equal to one. Colored dashed lines represent linear regressions between temperature and MCN for each dataset. The relationship between MCN and temperature is negative and statistically significantly for LMO (temperature sensitivity = -0.003 ± 0.001 ΔMCN/°C, p = 0.0005***), ANT (temperature sensitivity = -0.023 ± 0.002 ΔMCN/°C, p = 6.83e-15), and TARA (temperature sensitivity = -0.021 ± 0.002 ΔMCN/°C, p = 1.08e-12***), SPOT (temperature sensitivity = -0.056 ± 0.003 ΔMCN/°C, p < 2e-16***), while it is not significant in SOLA (temperature sensitivity = -0.007 ± 0.006 ΔMCN/°C, p = 0.273 n.s.). The relationship between MCN calculated excluding taxa with copy number = 1 and temperature is negative and statistically significantly for all datasets: LMO temperature sensitivity = -0.02 ± 0.003 ΔMCN/°C, p = 6.77e-12***, ANT temperature sensitivity = -0.016 ± 0.002 ΔMCN/°C, p = 1.1e-13***, TARA temperature sensitivity = -0.028 ± 0.003 ΔMCN/°C, p < 2e-16***, SOLA temperature sensitivity = -0.024 ± 0.001 ΔMCN/°C, p = 1.82e-09***, SPOT temperature sensitivity = -0.03 ± 0.003 ΔMCN/°C, p < 2e-16***.

Fig. S12.

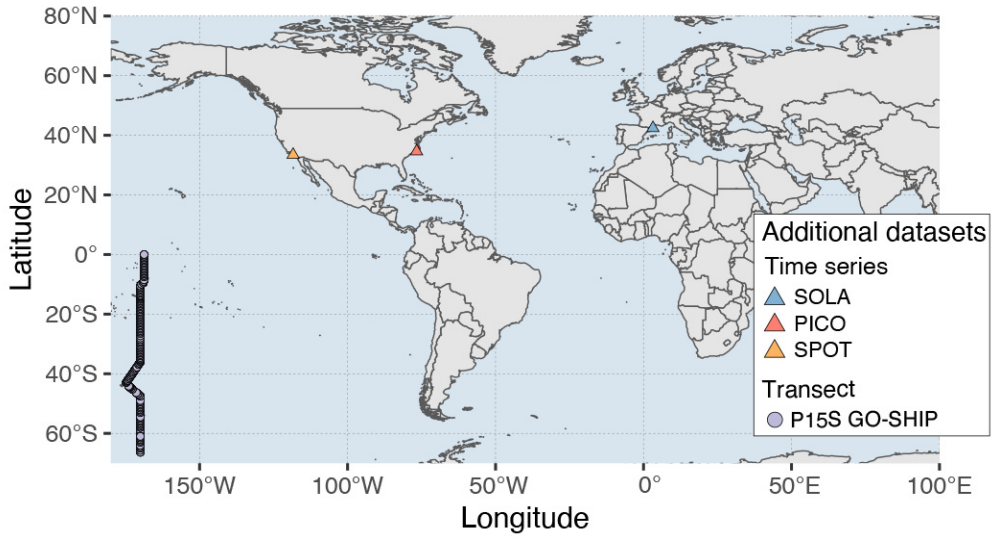

We considered a total of 7 datasets reporting the composition of marine bacterial communities. Map of the additional datasets included in the study.

Fig. S13.

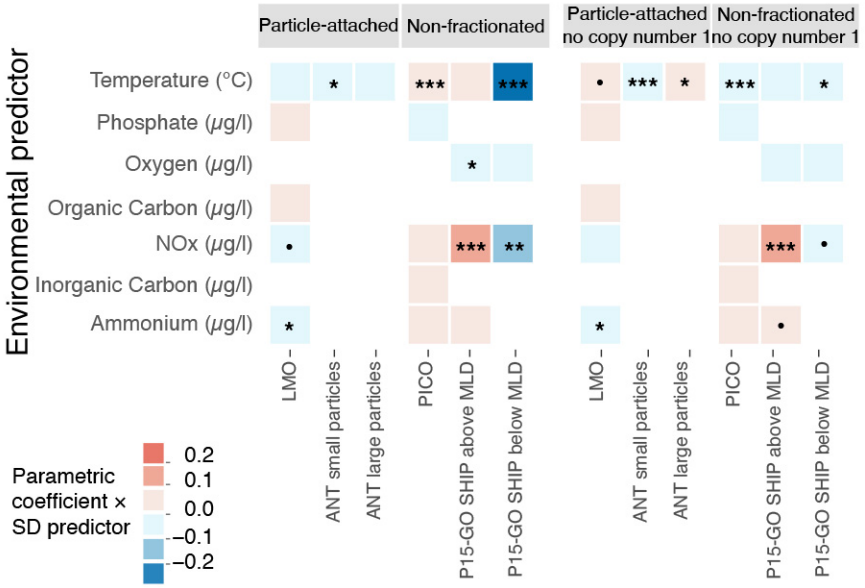

The effects of temperature on the distribution of fast and slow growers attached to particles are idiosyncratic. Summary of the results of the multi-parametric regression on MCN of particle-attached (available for LMO timeseries and ANT transect) and non-fractionated (available for PICO time series and P15 GO-SHIP transect) communities. Tile colors represent the magnitude and sign of the parametric coefficient estimated for each available environmental variable multiplied by its standard deviation. Statistical significance of the parametric coefficients estimated through the models is indicated by symbols: '***' 0.001 '**' 0.01 '*' 0.05 '.' 0.1 ' ' 1.

Fig. S14.

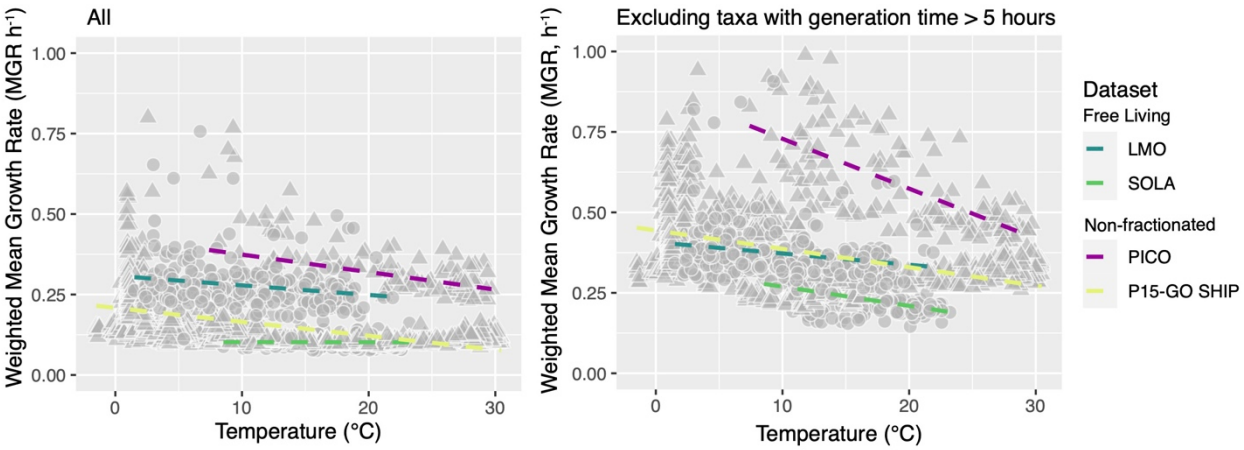

Figure S14. **Estimating the distribution of fast and slow growing taxa with an alternative method yields a negative relationship with temperature.** To test whether our conclusions depend on the method for estimating growth rates with rRNA copy number, we used another method based on codon usage bias (48) (this method is optimized for metagenomic datasets, although a 16S reference is available). The relationship between MGR (weighted mean growth rate, obtained from codon usage bias estimations) and temperature is negative and statistically significantly for LMO (temperature sensitivity = - 0.003±0.001 ΔMCN/°C, p = 0.0005***), PICO (temperature sensitivity = -0.005±0.001 ΔMCN/°C, p = 2.56e-07***), and P15 GO-SHIP (temperature sensitivity = -0.004 ± 0.0002 ΔMCN/°C, p < 2e-16 ***), while it is not significant in SOLA (temperature sensitivity = -0.00003 ± 0.0004 ΔMCN/°C, p = 0.947 n.s.). The relationship between MGR calculated excluding taxa with generation time longer than 5 hours (48) and temperature is negative and statistically significantly for all datasets: LMO temperature sensitivity = - 0.004 ± 0.001 ΔMCN/°C, p = 0.0005***, PICO temperature sensitivity = -0.017±0.001 ΔMCN/°C, p < 2e-16***, P15 GO-SHIP temperature sensitivity = -0.006 ± 0.0003 ΔMCN/°C, p < 2e-16***, SOLA temperature sensitivity = -0.006 ± 0.001 ΔMCN/°C, p = 1.82e-09***.

Table S1.

Effects of environmental variables on MCN of entire, copiotroph and heterotroph communities of all datasets included in the study. LMO, ANT, TARA, SOLA and SPOT comprise free-living communities, while PICO and P15 GO-SHIP include only non-fractionated samples. For LMO and ANT particle-attached communities are also available. *Organic carbon* is the dissolved fraction (DOC) in LMO and the particulate fraction (POC) in SPOT. *Light* measurements also differ between datasets: in SOLA it is measured as Day length (in hours); in PICO as insolation (kWh $m^{-2}d^{-1}$). Effects of environmental variables on MCN have been assessed using generalized additive (*gam*) or generalized additive mixed models (*gamm*). The latter were used when multiple sampling depths or stations were available the dataset, which were included in the random part of the model (ANT, SPOT, P15 GO-SHIP, and TARA). The intercept of the model and parametric coefficients (γ) for environmental variables are reported as Estimate (St. Error) Pr(>|t|). Significance codes: '***' 0.001 '**' 0.01 '*' 0.05 '.' 0.1 ' ' 1. Statistically significant parametric coefficients are highlighted in different shades of grey. Adjusted R^2 are included. Smooth terms and random terms are omitted.

		Intercept	*Temperature*	*Phosphate*	*Ammonium*	*Nitrate*	*Organic Carbon*	*Inorganic Carbon*	*Oxygen*	*Light*	*Chlorophyll a*	*Adj. R²*
All	LMO	2.966 (0.370) <2e-16 ***	- 0.031 (0.006) 1.82e-07***	- 0.023 (0.138) 0.868	- 0.082 (0.033) 0.015 *	- 0.068 (0.039) 0.806 .	- 0.001 (0.001) 0.111					0.259
	ANT	2.060 (0.078) <2e-16 ***	- 0.011 (0.005) 0.007 **									0.57
	TARA	1.766 (0.167) < 2e-16 ***	- 0.018 (0.005) 0.0008 ***	0.094 (0.047) 0.047 *		High colinearity (excluded)			0.001 (0.0004) 0.155			0.691
	SOLA	0.702 (0.170) <2e-16 ***	- 0.013 (0.007) 0.087 .	-0.388 (0.647) 0.550	-0.014 (0.080) 0.858	0.061 (0.023) 0.011 *				0.066 (0.012) 0.0609 ***		0.177
	SPOT	2.605 (0.139) < 2e-16 ***	-0.052 (0.011) 6.03e-06 ***						- 0.067 (0.213) 0.002 **			0.401
Copiotro	LMO	2.621 (0.341) 1.33e-12 ***	- 0.028 (0.006) 8.58e-06 ***	- 0.015 (0.130) 0.910	- 0.076 (0.031) 0.015 *	- 0.056 (0.036) 0.122	0.001 (0.001) 0.555					0.211
	ANT	2.754 (0.050)	- 0.005 (0.003) 0.082 .									0.563

phs		<2e-16 ***									
	TARA	2.104 (0.079) <2e-16 ***	- 0.023 (0.009) 0.008 **	0.099 (0.080) 0.216		High colline arity (exclud ed)		0.002 (0.00 1) 0.020 *			0.703
	SOLA	3.118 (0.174) <2e-16 ***	- 0.015 (0.008) 0.056 ·	0.088 (0.662) 0.894	-0.011 (0.082) 0.892	0.007 (0.02 4) 0.774			-0.023 (0.013) 0.072 ·		0.092
	SPOT	3.028 (0.074) < 2e-16 ***	-0.034 (0.009) 0.060 ** *					0.006 (0.01 7) 0.737			0.308
Heterotrophs	LMO	2.380 (0.441) 2.41e-07 ***	- 0.030 (0.009) 0.0007 ***	0.271 (0.193) 0.162	- 0.004 (0.043) 0.926	- 0.116 (0.05 2) 0.027 *	0.00 02 (0.00 1) 0.85 1			0.017 (0.030) 0.558	0.193
	ANT	2.104 (0.079) <2e-16 ***	- 0.015 (0.004) 0.0005 ***								0.601
	TARA	1.714 (0.165) <2e-16 ***	- 0.015 (0.005) 0.005 **	0.106 (0.046) 0.025 *				0.001 (0.00 04) 0.098 ·			0.671
	SOLA	0.102 (0.419) 0.807	0.002 (0.014) 0.881	-0.164 (0.730) 0.823	-0.007 (0.086) 0.938	0.045 (0.02 6) 0.082 ·			0.084 (0.034) 0.014 *	0.249 (0.060) 5.39e-05 ***	0.268
	SPOT	2.232 (0.350) 8e-07 ***	0.032 (0.014) 0.034 *	-0.666 (0.375) 0.087 ·		- 0.005 (0.03 6) 0.883	- 0.00 02 (0.00 03) 0.60 3	- 0.018 (0.03 9) 0.643		0.112 (0.030) 0.0009 ***	0.469
Particle	LMO	2.353 (0.52) 1.15e-05 ***	- 0.005 (0.009) 0.588	0.002 (0.198) 0.993	- 0.111 (0.047) 0.02 *	- 0.099 (0.05 5) 0.073 ·	0.00 1 (0.00 1) 0.59 5				0.041
	ANT small	2.356 (0.090) <2e-16 ***	- 0.010 (0.005) 0.03 *								0.426
	ANT large	2.213 (0.044) <2e-16 ***	- 0.003 (0.002) 0.11								0
Part	LMO	2.54 (0.245) < 2e-16 ***	- 0.014 (0.008) 0.08 ·	0.095 (0.192) 0.62	-0.113 (0.046) 0.015 *	- 0.077 (0.05	0.00 01 (0.00				0.09

						3) 0.15	1) 0.83			
copio	ANT small	2.842 (0.06) <2e-16 ***	-0.016 (0.003) 1.29e-06 ***							0.242
	ANT large	2.342 (0.039) <2e-16 ***	0.004 (0.002) 0.036 *							0.015
Non-fract	PICO	1.32(0.472) 0.006 **	0.011 (0.002) 1.78e-05 ***	- 0.344 (0.443) 0.439	0 (0) 0.942	0.021 (0.119) 0.858	0.0001 (0.0002) 0.618		High collinearity (excluded)	0.127
	P15-GO SHIP above MLD	1.645 (0.146) <2e-16 ***	0.002 (0.002) 0.496		0.054 (0.051) 0.286	0.010 (0.002) 1.33e-09 ***		-0.001 (0.0004) 0.015 *		0.364
	P15-GO SHIP below MLD	2.162 (0.382) 1.17e-15 ***	- 0.082 (0.010) 4.07e-14 ***			- 0.025 (0.007) 0.0004 ***		- 0.001 (0.001) 0.032 *		0.478
Non-fract copio	PICO	1.473(0.173) 2.13e-14***	- 0.007 (0.001) 2.08e-12 ***	-0.085 (0.163) 0.6	0 (0) 0.496	0.052 (0.043) 0.232	0.0004 (0.0001) ***		High collinearity (excluded)	0.315
	P15-GO SHIP above MLD	2.412 (0.168) < 2e-16 ***	- 0.0003 (0.003) 0.917		0.110 (0.058) 0.060 ·	0.012 (0.002) 2.92e-10 ***		- 0.001 (0.0005) 0.246		0.624
	P15-GO SHIP below MLD	3.650 (0.0470) 4.54e-14 ***	- 0.032 (0.013) 0.013 *			- 0.016 (0.009) 0.062 ·		- 0.001 (0.0001) 0.120		0.245

REFERENCES AND NOTES

1. P. G. Falkowski, T. Fenchel, E. F. Delong, The microbial engines that drive earth's biogeochemical cycles. *Science* **320**, 1034–1039 (2008).

2. C. B. Field, M. J. Behrenfeld, J. T. Randerson, P. Falkowski, Primary production of the biosphere: Integrating terrestrial and oceanic components. *Science* **281**, 237–240 (1998).

3. C. E. T. Chow, R. Sachdeva, J. A. Cram, J. A. Steele, D. M. Needham, A. Patel, A. E. Parada, J. A. Fuhrman, Temporal variability and coherence of euphotic zone bacterial communities over a decade in the Southern California Bight. *ISME J.* **7**, 2259–2273 (2013).

4. C. S. Ward, C.-M. Yung, K. M. Davis, S. K. Blinebry, T. C. Williams, Z. I. Johnson, D. E. Hunt, Annual community patterns are driven by seasonal switching between closely related marine bacteria. *ISME J.* **11**, 1412–1422 (2017).

5. M. V. Lindh, J. Sjöstedt, A. F. Andersson, F. Baltar, L. W. Hugerth, D. Lundin, S. Muthusamy, C. Legrand, J. Pinhassi, Disentangling seasonal bacterioplankton population dynamics by high-frequency sampling. *Environ. Microbiol.* **17**, 2459–2476 (2015).

6. C. Bunse, J. Pinhassi, Marine bacterioplankton seasonal succession dynamics. *Trends Microbiol.* **25**, 494–505 (2017).

7. A. S. Amend, T. A. Oliver, L. A. Amaral-Zettler, A. Boetius, J. A. Fuhrman, M. C. Horner-Devine, S. M. Huse, D. B. M. Welch, A. C. Martiny, A. Ramette, L. Zinger, M. L. Sogin, J. B. H. Martiny, Macroecological patterns of marine bacteria on a global scale. *J. Biogeogr.* **40**, 800–811 (2013).

8. S. Sunagawa, L. P. Coelho, S. Chaffron, J. R. Kultima, K. Labadie, G. Salazar, B. Djahanschiri, G. Zeller, D. R. Mende, A. Alberti, F. M. Cornejo-Castillo, P. I. Costea, C. Cruaud, F. D'Ovidio, S. Engelen, I. Ferrera, J. M. Gasol, L. Guidi, F. Hildebrand, F. Kokoszka, C. Lepoivre, G. Lima-Mendez, J. Poulain, B. T. Poulos, M. Royo-Llonch, H. Sarmento, S. Vieira-Silva, C. Dimier, M. Picheral, S. Searson, S. Kandels-Lewis, E. Boss, M. Follows, L. Karp-Boss, U. Krzic, E. G. Reynaud, C. Sardet, M. Sieracki, D. Velayoudon, C.

Bowler, C. De Vargas, G. Gorsky, N. Grimsley, P. Hingamp, D. Iudicone, O. Jaillon, F. Not, H. Ogata, S. Pesant, S. Speich, L. Stemmann, M. B. Sullivan, J. Weissenbach, P. Wincker, E. Karsenti, J. Raes, S. G. Acinas, P. Bork, Structure and function of the global ocean microbiome. *Science* **348**, 1261359 (2015).

9. S. De Monte, A. Soccodato, S. Alvain, F. D'Ovidio, Can we detect oceanic biodiversity hotspots from space? *ISME J.* **7**, 2054–2056 (2013).

10. S. C. Doney, Oceanography: Plankton in a warmer world. *Nature* **444**, 695–696 (2006).

11. D. J. Richter, R. Watteaux, T. Vannier, J. Leconte, P. Frémont, G. Reygondeau, N. Maillet, N. Henry, G. Benoit, O. Da Silva, T. O. Delmont, A. Fernàndez-Guerra, S. Suweis, R. Narci, C. Berney, D. Eveillard, F. Gavory, L. Guidi, K. Labadie, E. Mahieu, J. Poulain, S. Romac, S. Roux, C. Dimier, S. Kandels, M. Picheral, S. Searson, T. O. Coordinators, S. Pesant, J.-M. Aury, J. R. Brum, C. Lemaitre, E. Pelletier, P. Bork, S. Sunagawa, F. Lombard, L. Karp-Boss, C. Bowler, M. B. Sullivan, E. Karsenti, M. Mariadassou, I. Probert, P. Peterlongo, P. Wincker, C. de Vargas, M. R. d'Alcalà, D. Iudicone, O. Jaillon, Genomic evidence for global ocean plankton biogeography shaped by large-scale current systems. *bioRxiv* 867739 (2020). https://doi.org/10.1101/867739

12. T. Dai, D. Wen, C. T. Bates, L. Wu, X. Guo, S. Liu, Y. Su, J. Lei, J. Zhou, Y. Yang, Nutrient supply controls the linkage between species abundance and ecological interactions in marine bacterial communities. *Nat. Commun.* **13**, 1–9 (2022).

13. S. J. Biller, P. M. Berube, D. Lindell, S. W. Chisholm, Prochlorococcus: The structure and function of collective diversity. *Nat. Rev. Microbiol.* **13**, 13–27 (2015).

14. J. B. H. Martiny, S. E. Jones, J. T. Lennon, A. C. Martiny, Microbiomes in light of traits: A phylogenetic perspective. *Science* **350**, aac9323 (2015).

15. E. Litchman, K. F. Edwards, C. A. Klausmeier, Microbial resource utilization traits and trade-offs: Implications for community structure, functioning, and biogeochemical impacts at present and in the future. *Front. Microbiol.* **6**, 254 (2015).

16. P. B. Reich, The world-wide ‘fast–slow’ plant economics spectrum: A traits manifesto. *J. Ecol.* **102**, 275–301 (2014).

17. A. C. Siqueira, W. Kiessling, D. R. Bellwood, Fast-growing species shape the evolution of reef corals. *Nat. Commun.* **13**, 1–8 (2022).

18. P. J. Edmunds, M. Adjeroud, M. L. Baskett, I. B. Baums, A. F. Budd, R. C. Carpenter, N. S. Fabina, T. Y. Fan, E. C. Franklin, K. Gross, X. Han, L. Jacobson, J. S. Klaus, T. R. McClanahan, J. K. O’Leary, M. J. H. Van Oppen, X. Pochon, H. M. Putnam, T. B. Smith, M. Stat, H. Sweatman, R. Van Woesik, R. D. Gates, Persistence and change in community composition of reef corals through present, past, and future climates. *PLOS ONE* **9**, e107525 (2014).

19. D. L. Kirchman, Growth rates of microbes in the oceans. *Ann. Rev. Mar. Sci.* **8**, 285–309 (2016).

20. J. A. Klappenbach, J. M. Dunbar, T. M. Schmidt, rRNA operon copy number reflects ecological strategies of bacteria. *Appl. Environ. Microbiol.* **66**, 1328–1333 (2000).

21. E. R. Pianka, On r- and K-selection. *Am. Nat.* **104**, 592–597 (1970).

22. D. Reznick, M. J. Bryant, F. Bashey, r- and K-selection revisited: The role of population regulation in life-history evolution. *Special Feature Ecol.* **83**, 1509–1520 (2002).

23. V. M. Savage, J. F. Gillooly, J. H. Brown, G. B. West, E. L. Charnov, Effects of body size and temperature on population growth. *Am. Nat.* **163**, 429–441 (2004).

24. B. D. Knapp, K. C. Huang, The Effects of Temperature on Cellular Physiology. *Annu. Rev. Biophys.* **51**, 499–526 (2022).

25. F. M. Lauro, D. McDougald, T. Thomas, T. J. Williams, S. Egan, S. Rice, M. Z. DeMaere, L. Ting, H. Ertan, J. Johnson, S. Ferriera, A. Lapidus, I. Anderson, N. Kyrpides, A. C. Munk, C. Detter, C. S. Han, M. V. Brown, F. T. Robb, S. Kjelleberg, R. Cavicchioli, The genomic basis of trophic strategy in marine bacteria. *Proc. Natl. Acad. Sci. U.S.A.* **106**, 15527–15533 (2009).

26. B. S. Stevenson, T. M. Schmidt, Life history implications of rRNA gene copy number in Escherichia coli. *Appl. Environ. Microbiol.* **70**, 6670–6677 (2004).

27. S. J. Giovannoni, J. Cameron Thrash, B. Temperton, Implications of streamlining theory for microbial ecology. *ISME J.* **8**, 1553–1565 (2014).

28. N. Norris, N. M. Levine, V. I. Fernandez, R. Stocker, Mechanistic model of nutrient uptake explains dichotomy between marine oligotrophic and copiotrophic bacteria. *PLoS Comput. Biol.* **17**, e1009023 (2021).

29. S. M. Neuenschwander, R. Ghai, J. Pernthaler, M. M. Salcher, Microdiversification in genome-streamlined ubiquitous freshwater Actinobacteria. *ISME J.* **12**, 185–198 (2018).

30. L. Wu, Y. Yang, S. Chen, Z. Jason Shi, M. Zhao, Z. Zhu, S. Yang, Y. Qu, Q. Ma, Z. He, J. Zhou, Q. He, Microbial functional trait of rRNA operon copy numbers increases with organic levels in anaerobic digesters. *ISME J.* **11**, 2874–2878 (2017).

31. D. R. Nemergut, J. E. Knelman, S. Ferrenberg, T. Bilinski, B. Melbourne, L. Jiang, C. Violle, J. L. Darcy, T. Prest, S. K. Schmidt, A. R. Townsend, Decreases in average bacterial community rRNA operon copy number during succession. *ISME J.* **10**, 1147–1156 (2015).

32. T. Dai, Y. Zhao, D. Ning, B. Huang, Q. Mu, Y. Yang, D. Wen, Dynamics of coastal bacterial community average ribosomal RNA operon copy number reflect its response and sensitivity to ammonium and phosphate. *Environ. Pollut.* **260**, 113971 (2020).

33. M. K. Thomas, C. T. Kremer, C. A. Klausmeier, E. Litchman, A global pattern of thermal adaptation in marine phytoplankton. *Science* **338**, 1085–1088 (2012).

34. B. R. K. Roller, S. F. Stoddard, T. M. Schmidt, Exploiting rRNA operon copy number to investigate bacterial reproductive strategies. *Nat. Microbiol.* **1**, 1–7 (2016).

35. S. Vieira-Silva, E. P. C. Rocha, The systemic imprint of growth and its uses in ecological (Meta)Genomics. *PLOS Genet.* **6**, e1000808 (2010).

36. S. F. Stoddard, B. J. Smith, R. Hein, B. R. K. Roller, T. M. Schmidt, rrnDB: Improved tools for interpreting rRNA gene abundance in bacteria and archaea and a new foundation for future development. *Nucleic Acids Res.* **43**, D593–D598 (2015).

37. M. Milici, J. Tomasch, M. L. Wos-Oxley, J. Decelle, R. Jáuregui, H. Wang, Z.-L. Deng, I. Plumeier, H.-A. Giebel, T. H. Badewien, M. Wurst, D. H. Pieper, M. Simon, I. Wagner-Döbler, Bacterioplankton biogeography of the atlantic ocean: A case study of the distance-decay relationship. *Front. Microbiol.* **7**, 590 (2016).

38. M. Milici, Z.-L. Deng, J. Tomasch, J. Decelle, M. L. Wos-Oxley, H. Wang, R. Jáuregui, I. Plumeier, H.-A. Giebel, T. H. Badewien, M. Wurst, D. H. Pieper, M. Simon, I. Wagner-Döbler, Co-occurrence analysis of microbial taxa in the atlantic ocean reveals high connectivity in the free-living bacterioplankton. *Front. Microbiol.* **0**, 649 (2016).

39. M. Milici, J. Tomasch, M. L. Wos-Oxley, H. Wang, R. Jáuregui, A. Camarinha-Silva, Z. L. Deng, I. Plumeier, H. A. Giebel, M. Wurst, D. H. Pieper, M. Simon, I. Wagner-Döbler, Low diversity of planktonic bacteria in the tropical ocean. *Sci. Rep.* **6**, 1–9 (2016).

40. S. Lax, C. I. Abreu, J. Gore, Higher temperatures generically favour slower-growing bacterial species in multispecies communities. *Nat Ecol Evol.* **4**, 560–567 (2020).

41. C. A. Suttle, Marine viruses — Major players in the global ecosystem. *Nat. Rev. Microbiol.* **5**, 801–812 (2007).

42. O. Sánchez, I. Ferrera, I. Mabrito, C. R. Gazulla, M. Sebastián, A. Auladell, C. Marín-Vindas, C. Cardelús, I. Sanz-Sáez, M. C. Pernice, C. Marrasé, M. M. Sala, J. M. Gasol, Seasonal impact of grazing, viral mortality, resource availability and light on the group-specific growth rates of coastal Mediterranean bacterioplankton. *Sci. Rep.* **10**, 1–15 (2020).

43. J. A. Fuhrman, R. T. Noble, Viruses and protists cause similar bacterial mortality in coastal seawater. *Limnol. Oceanogr.* **40**, 1236–1242 (1995).

44. J. A. Boras, M. M. Sala, E. Vázquez-Domínguez, M. G. Weinbauer, D. Vaqué, Annual changes of bacterial mortality due to viruses and protists in an oligotrophic coastal environment (NW Mediterranean). *Environ. Microbiol.* **11**, 1181–1193 (2009).

45. L. J. Ustick, A. A. Larkin, C. A. Garcia, N. S. Garcia, M. L. Brock, J. A. Lee, N. A. Wiseman, J. Keith Moore, A. C. Martiny, Metagenomic analysis reveals global-scale patterns of ocean nutrient limitation. *Science* **372**, 287–291 (2021).

46. S. J. Giovannoni, SAR11 bacteria: The most abundant plankton in the oceans. *Ann. Rev. Mar. Sci.* **9**, 231–255 (2017).

47. S. J. Giovannoni, H. J. Tripp, S. Givan, M. Podar, K. L. Vergin, D. Baptista, L. Bibbs, J. Eads, T. H. Richardson, M. Noordewier, M. S. Rappé, J. M. Short, J. C. Carrington, E. J. Mathur, Genome streamlining in a cosmopolitan oceanic bacterium. *Science* **309**, 1242–1245 (2005).

48. S. Lambert, M. Tragin, J. C. Lozano, J. F. Ghiglione, D. Vaulot, F. Y. Bouget, P. E. Galand, Rhythmicity of coastal marine picoeukaryotes, bacteria and archaea despite irregular environmental perturbations. *ISME J.* **13**, 388–401 (2019).

49. A. E. Parada, J. A. Fuhrman, Marine archaeal dynamics and interactions with the microbial community over 5 years from surface to seafloor. *ISME J.* **11**, 2510–2525 (2017).

50. P. Flombaum, J. L. Gallegos, R. A. Gordillo, J. Rincón, L. L. Zabala, N. Jiao, D. M. Karl, W. K. W. Li, M. W. Lomas, D. Veneziano, C. S. Vera, J. A. Vrugt, A. C. Martiny, Present and future global distributions of the marine Cyanobacteria Prochlorococcus and Synechococcus. *Proc. Natl. Acad. Sci. U.S.A.* **110**, 9824–9829 (2013).

51. L. R. Moore, R. Goericke, S. W. Chisholm, Comparative physiology of Synechococcus and Prochlorococcus: Influence of light and temperature on growth, pigments, fluorescence and absorptive properties. *Mar. Ecol. Prog. Ser.* **116**, 259–276 (1995).

52. B. L. Fowler, M. G. Neubert, K. R. Hunter-Cevera, R. J. Olson, A. Shalapyonok, A. R. Solow, H. M. Sosik, Dynamics and functional diversity of the smallest phytoplankton on the Northeast US Shelf. *Proc. Natl. Acad. Sci. U.S.A.* **117**, 12215–12221 (2020).

53. K. M. DeAngelis, G. Pold, B. D. Topçuoğlu, L. T. A. van Diepen, R. M. Varney, J. L. Blanchard, J. Melillo, S. D. Frey, Long-term forest soil warming alters microbial communities in temperate forest soils. *Front. Microbiol.* **6**, 104 (2015).

54. J. M. Melillo, S. D. Frey, K. M. DeAngelis, W. J. Werner, M. J. Bernard, F. P. Bowles, G. Pold, M. A. Knorr, A. S. Grandy, Long-term pattern and magnitude of soil carbon feedback to the climate system in a warming world. *Science* **358**, 101–105 (2017).

55. A. Söllinger, J. Séneca, M. Borg Dahl, L. L. Motleleng, J. Prommer, E. Verbruggen, B. D. Sigurdsson, I. Janssens, J. Peñuelas, T. Urich, A. Richter, A. T. Tveit, Down-regulation of the bacterial protein biosynthesis machinery in response to weeks, years, and decades of soil warming. *Sci. Adv.* **8**, 3230 (2022).

56. T. Pfeiffer, S. Schuster, S. Bonhoeffer, Cooperation and competition in the evolution of ATP-producing pathways. *Science* **292**, 504–507 (2001).

57. R. H. MacArthur, E. O. Wilson, *The Theory of Island biogeography* (Princeton University Press, 1967).

58. J. L. Weissman, S. Hou, J. A. Fuhrman, Estimating maximal microbial growth rates from cultures, metagenomes, and single cells via codon usage patterns. *Proc. Natl. Acad. Sci. U.S.A.* **118**, e2016810118 (2021).

59. P. Chesson, Mechanisms of maintenance of species diversity. *Annu. Rev. Ecol. Syst.* **31**, 343–366 (2000).

60. A. D. Letten, P. J. Ke, T. Fukami, Linking modern coexistence theory and contemporary niche theory. *Ecol. Monogr.* **87**, 161–177 (2017).

61. C. I. Abreu, J. Friedman, V. L. Andersen Woltz, J. Gore, Mortality causes universal changes in microbial community composition. *Nat. Commun.* **10**, 1–9 (2019).

62. R. Cavicchioli, W. J. Ripple, K. N. Timmis, F. Azam, L. R. Bakken, M. Baylis, M. J. Behrenfeld, A. Boetius, P. W. Boyd, A. T. Classen, T. W. Crowther, R. Danovaro, C. M. Foreman, J. Huisman, D. A. Hutchins, J. K. Jansson, D. M. Karl, B. Koskella, D. B. Mark Welch, J. B. H. Martiny, M. A. Moran, V. J. Orphan, D. S. Reay, J. V. Remais, V. I. Rich, B. K. Singh, L. Y. Stein, F. J. Stewart, M. B. Sullivan, M. J. H. van Oppen, S. C. Weaver, E. A. Webb, N. S. Webster, Scientists' warning to humanity: Microorganisms and climate change. *Nat. Rev. Microbiol.* **17** 569–586 (2019).

63. S. C. Doney, M. Ruckelshaus, J. Emmett Duffy, J. P. Barry, F. Chan, C. A. English, H. M. Galindo, J. M. Grebmeier, A. B. Hollowed, N. Knowlton, J. Polovina, N. N. Rabalais, W. J. Sydeman, L. D. Talley, Climate change impacts on marine ecosystems. *Ann. Rev. Mar. Sci.* **4**, 11–37 (2012).

64. C. Bunse, S. Israelsson, F. Baltar, M. Bertos-Fortis, E. Fridolfsson, C. Legrand, E. Lindehoff, M. V. Lindh, S. Martínez-García, J. Pinhassi, High frequency multi-year variability in baltic sea microbial plankton stocks and activities. *Front. Microbiol.* **10**, 3296 (2019).

65. K. H. Boström, K. Simu, Å. Hagström, L. Riemann, Optimization of DNA extraction for quantitative marine bacterioplankton community analysis. *Limnol. Oceanogr. Methods* **2**, 365–373 (2004).

66. C. Bunse, D. Lundin, C. M. G. Karlsson, N. Akram, M. Vila-Costa, J. Palovaara, L. Svensson, K. Holmfeldt, J. M. González, E. Calvo, C. Pelejero, C. Marrasé, M. Dopson, J. M. Gasol, J. Pinhassi, Response of marine bacterioplankton pH homeostasis gene expression to elevated CO_2. *Nat. Clim. Chang.* **6**, 483–487 (2016).

67. D. P. R. Herlemann, M. Labrenz, K. Jürgens, S. Bertilsson, J. J. Waniek, A. F. Andersson, Transitions in bacterial communities along the 2000 km salinity gradient of the Baltic Sea. *ISME J.* **5**, 1571–1579 (2011).

68. D. Straub, N. Blackwell, A. Langarica-Fuentes, A. Peltzer, S. Nahnsen, S. Kleindienst, Interpretations of environmental microbial community studies are biased by the selected 16S rRNA (Gene) amplicon sequencing pipeline. *Front. Microbiol.* **11**, 2652 (2020).

69. B. J. Callahan, P. J. McMurdie, M. J. Rosen, A. W. Han, A. J. A. Johnson, S. P. Holmes, DADA2: High-resolution sample inference from Illumina amplicon data. *Nat. Methods* **13**, 581–583 (2016).

70. C. Quast, E. Pruesse, P. Yilmaz, J. Gerken, T. Schweer, P. Yarza, J. Peplies, F. O. Glöckner, The SILVA ribosomal RNA gene database project: Improved data processing and web-based tools. *Nucleic Acids Res.* **41**, D590–D596 (2013).

71. F. M. Ibarbalz, N. Henry, M. C. Brandão, S. Martini, G. Busseni, H. Byrne, L. P. Coelho, H. Endo, J. M. Gasol, A. C. Gregory, F. Mahé, J. Rigonato, M. Royo-Llonch, G. Salazar, I. Sanz-Sáez, E. Scalco, D. Soviadan, A. A. Zayed, A. Zingone, K. Labadie, J. Ferland, C. Marec, S. Kandels, M. Picheral, C. Dimier, J. Poulain, S. Pisarev, M. Carmichael, S. Pesant, S. G. Acinas, M. Babin, P. Bork, E. Boss, C. Bowler, G. Cochrane, C. de Vargas, M. Follows, G. Gorsky, N. Grimsley, L. Guidi, P. Hingamp, D. Iudicone, O. Jaillon, S. Kandels, L. Karp-Boss, E. Karsenti, F. Not, H. Ogata, S. Pesant, N. Poulton, J. Raes, C. Sardet, S. Speich, L. Stemmann, M. B. Sullivan, S. Sunagawa, P. Wincker, M. Babin, E. Boss, D. Iudicone, O. Jaillon, S. G. Acinas, H. Ogata, E. Pelletier, L. Stemmann, M. B. Sullivan, S. Sunagawa, L. Bopp, C. de Vargas, L. Karp-Boss, P. Wincker, F. Lombard, C. Bowler, L. Zinger, Global trends in marine plankton diversity across kingdoms of life. *Cell* **179**, 1084–1097.e21 (2019).

72. S. Sunagawa, S. G. Acinas, P. Bork, C. Bowler, D. Eveillard, G. Gorsky, L. Guidi, D. Iudicone, E. Karsenti, F. Lombard, H. Ogata, S. Pesant, M. B. Sullivan, P. Wincker, C. de Vargas, Tara Oceans: Towards global ocean ecosystems biology. *Nat. Rev. Microbiol.* **18**, 428–445 (2020).

73. E. J. Raes, L. Bodrossy, J. Van De Kamp, A. Bissett, M. Ostrowski, M. V. Brown, S. L. S. Sow, B. Sloyan, A. M. Waite, Oceanographic boundaries constrain microbial diversity gradients in the south pacific ocean. *Proc. Natl. Acad. Sci. U.S.A.* **115**, E8266–E8275 (2018).

74. T. M. Huete-Stauffer, N. Arandia-Gorostidi, L. Díaz-Pérez, X. A. G. Morán, Temperature dependences of growth rates and carrying capacities of marine bacteria depart from metabolic theoretical predictions. *FEMS Microbiol. Ecol.* **91**, fiv111 (2015).

75. N. Arandia-Gorostidi, T. M. Huete-Stauffer, L. Alonso-Sáez, X. A. Xosé, Testing the metabolic theory of ecology with marine bacteria: Different temperature sensitivity of major phylogenetic groups during the spring phytoplankton bloom. *Environ. Microbiol.* **19**, 4493–4505 (2017).

76. A. F. Zuur, E. N. Ieno, N. J. Walker, A. A. Saveliev, G. M. Smith, *Mixed Effects Models and Extensions in Ecology with R* (2009), vol. 1.

77. A. Guisan, T. C. Edwards, T. Hastie, Generalized linear and generalized additive models in studies of species distributions: Setting the scene. *Ecol. Model.* **157**, 89–100 (2002).

78. S. N. Wood, Fast stable restricted maximum likelihood and marginal likelihood estimation of semiparametric generalized linear models. *J. R. Stat. Soc. Series B Stat. Methodol.* **73**, 3–36 (2011).

79. S. N. Wood, Thin plate regression splines. *J. R. Stat. Soc. Series B Stat. Methodol.* **65**, 95–114 (2003).

80. G. Wahba, Spline Interpolation and Smoothing on the Sphere. *SIAM J. Sci. Stat. Comput.* **2**, 5–16 (1981).

81. D. Lüdecke, M. S. Ben-Shachar, I. Patil, P. Waggoner, D. Makowski, performance: An R package for assessment, comparison and testing of statistical models. *J. Open Source Softw.* **6**, 3139 (2021).

82. R. McElreath, *Statistical rethinking: A Bayesian course with examples in R and Stan.* (Chapman and Hall/CRC, ed. 2, 2020).

83. D. A. Ratkowsky, J. Olley, T. A. McMeekin, A. Ball, Relationship between temperature and growth rate of bacterial cultures. *J. Bacteriol.* **149**, 1 (1982).